

## Synthesis of information on aerosol optical properties

Hongqing Liu,<sup>1</sup> R. T. Pinker,<sup>1</sup> M. Chin,<sup>2</sup> B. Holben,<sup>3</sup> and L. Remer<sup>2</sup>

Received 1 April 2007; revised 4 November 2007; accepted 14 December 2007; published 10 April 2008.

[1] In a previous study (Liu et al., 2005) obtained are global scale estimates of aerosol optical depth at  $0.55 \mu\text{m}$  based on spatial and temporal variation patterns from models and satellite observations, regulated by the Aerosol Robotic Network (AERONET) measurements. In this study an approach is developed to obtain information on global distribution of the single scattering albedo ( $\omega_0$ ), the asymmetry parameter ( $g$ ), and the normalized extinction coefficient over shortwave (SW) spectrum. Since space observations of  $\omega_0$  are in early stages of development and none are available for  $g$ , first an approach was developed to infer them from relevant information from the Global Ozone Chemistry Aerosol Radiation and Transport (GOCART) model, Moderate Resolution Imaging Spectroradiometer (MODIS) and AERONET retrievals. The single scattering albedo is generated by extending GOCART  $\omega_0$  at  $0.55 \mu\text{m}$  to the entire SW spectrum using spectral dependence derived from AERONET retrievals. The asymmetry parameter over the solar spectrum is derived from the MODIS Ångström wavelength exponent, utilizing a relationship based on AERONET almucantar observations. The normalized extinction coefficient is estimated from the MODIS Ångström wavelength exponent. The methodology was implemented as a “proof of concept” with one year of data. The approach described here is a step in preparedness for utilizing information from new observing systems (e.g., MISR, A-Train constellation) when available. The impact of the newly derived information on the quality of satellite based estimates of surface radiative fluxes was evaluated and is presented by Liu and Pinker (2008).

**Citation:** Liu, H., R. T. Pinker, M. Chin, B. Holben, and L. Remer (2008), Synthesis of information on aerosol optical properties, *J. Geophys. Res.*, 113, D07206, doi:10.1029/2007JD008735.

### 1. Introduction

[2] Information on aerosol optical properties at different spatial and temporal scales is becoming available from several sources. They include chemical transport models, satellite and ground observations and there is a need to synthesize them into useful information for large scale radiative transfer calculations. Natural as well as anthropogenic aerosols have a significant yet largely uncertain effect on the Earth radiation balance [Intergovernmental Panel on Climate Change, 2001]. Their potential to increase reflected solar radiation and the resultant modulation of top of the atmosphere radiation budget has motivated numerous investigations in the climate and radiation research communities [Charlson et al., 1992; Kiehl and Briegleb, 1993; Boucher and Anderson, 1995; Schwartz, 1996; Hansen et al., 1997]. Recent observations revealed a significant decrease in surface solar heating due to the presence of absorbing aerosols, which might slow down the hydrological cycle and affect

atmospheric dynamics [Satheesh and Ramanathan, 2000; Russell et al., 1999; Bush and Valero, 2003]. Quantification of the influence of aerosols on the shortwave radiation budget requires a complete global characterization of aerosol concentration and radiative properties. For this purpose, an extension of a previous study [Liu et al., 2005] on the global estimate of aerosol optical depth at  $0.55 \mu\text{m}$  is undertaken in this work. Derived is a global description of aerosol intensive optical properties (single scattering albedo, asymmetry parameter and normalized extinction coefficient) over the entire solar spectrum by synthesizing data from the MODerate-resolution Imaging Spectroradiometer (MODIS) satellite retrievals, AERosol RObotic NETwork (AERONET) ground observations and Global Ozone Chemistry Aerosol Radiation Transport (GOCART) model simulations.

[3] Aerosol representation in shortwave radiative transfer calculation is complicated due to the fact that multiple parameters are needed for a “radiatively complete” description of their properties. Three parameters/functions are the fundamental inputs to such models: (1) Aerosol optical depth ( $\tau$ ), an extensive state parameter associated with aerosol column amount. Spectral variation of  $\tau$  is usually characterized by Ångström exponent ( $\alpha$ ), which describes the slope of  $\log \tau$  versus  $\log \lambda$ ; (2) Single scattering albedo ( $\omega_0$ ), defined as the ratio of scattering optical depth to total optical depth (scattering plus absorption); (3) Scattering phase function, describes the angular distribution of scat-

<sup>1</sup>Department of Atmospheric and Oceanic Science, University of Maryland, College Park, Maryland, USA.

<sup>2</sup>NASA Goddard Space Flight Center, Atmospheres Lab, Greenbelt, Maryland, USA.

<sup>3</sup>NASA, Goddard Space Flight Center, Biospheric Sciences Branch, Greenbelt, Maryland, USA.

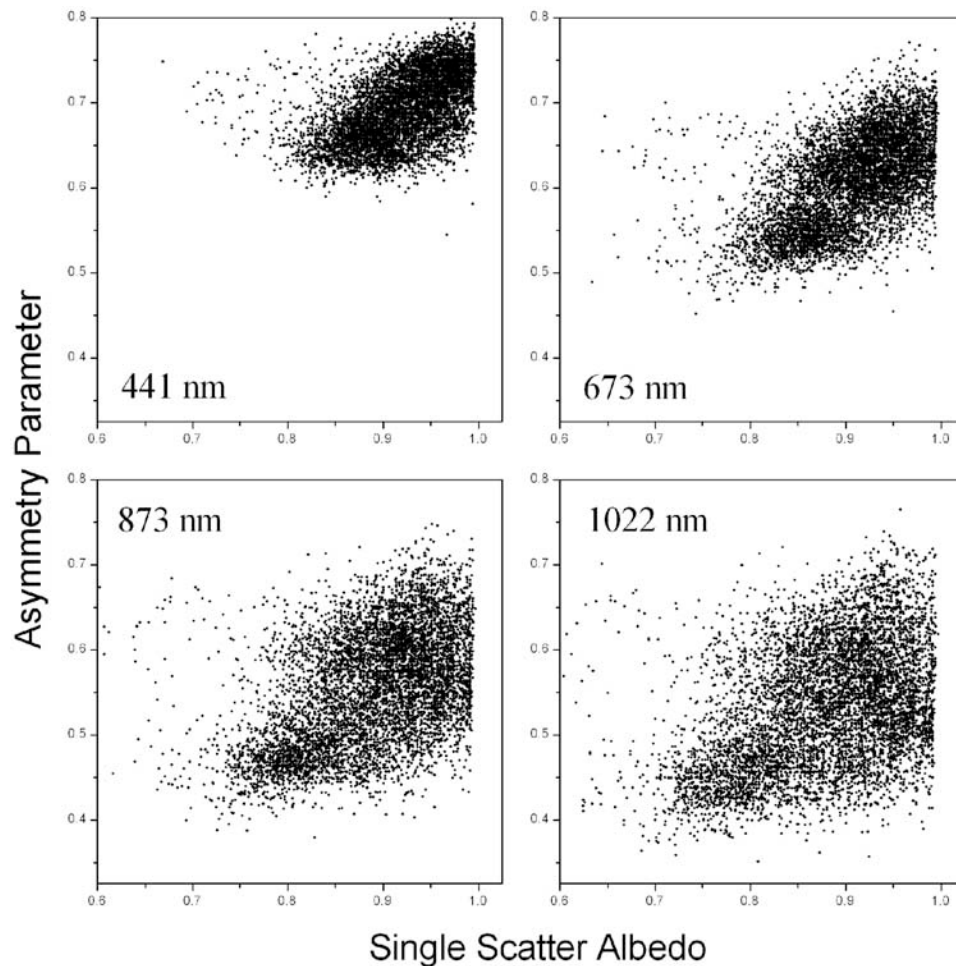


**Figure 1.** Scatterplots of aerosol single scattering albedo and asymmetry parameter for four wavelengths. Data used are derived from AERONET almucantar measurements over more than 10 years (1993–2003).

tered radiation and usually, asymmetry parameter ( $g$ ), the first moment of the phase function, is employed to characterize the aerosol scattering properties in flux calculations. The asymmetry parameter and single scattering albedo are regarded as intensive state parameters independent on the amount of aerosols present.

[4] Further complexity of aerosol characterization is related to spatial, temporal and spectral variability of these parameters. On the basis of multiyear AERONET Sun photometer measurements, *Holben et al.* [2001] identified a large variation in aerosol optical depth (AOD) and its wavelength dependence (Ångström exponent) over a wide range of aerosol regimes. To illustrate variability in  $\omega_0$  and  $g$ , we created scatterplots of  $\omega_0$  versus  $g$  at four wavelengths (0.44, 0.67, 0.87, and 1.02  $\mu\text{m}$ ) as shown in Figure 1. More than 6000 instantaneous almucantar retrievals from the global AERONET network during 1993–2003 were used [*Dubovik et al.*, 2002a]. As evident, variations associated with absorption and scattering are widely spread and hinder an unambiguous classification of ambient aerosols into radiatively distinctive types. Consequently, a limited number of aerosol models are inadequate to describe the complexity of global aerosol properties.

[5] In what follows, data used in this study are introduced in section 2. Methodologies developed to derive global  $\omega_0$ ,  $g$  and normalized extinction coefficient are presented in section 3. Sensitivity tests of the effect of uncertainties in  $\omega_0$  and  $g$  on surface downward SW fluxes are performed in section 4. A summary is presented in section 5.

## 2. Data Used

### 2.1. Model Simulations

[6] Aerosol radiative characteristics are determined by their microphysical (size distribution and shape) and chemical (composition) properties. Numerous models have been developed to simulate the physical and chemical processes involved in the short and complicated aerosol life cycles. Aerosol formation, removal, primary physical/chemical processes and the resulting size distribution are discussed by *Whitby and Cantrell* [1975].

[7] Lateral and vertical transport by the atmospheric circulation; hygroscopic growth by uptake of water vapor; heterogeneous chemistry on particle surface and interactions with other aerosols and clouds, need to be accounted for.

[8] Using the simulated aerosol concentrations and microphysical/chemical properties, radiative properties can be

estimated based on electromagnetic or optical models [Mie, 1908; Mishchenko *et al.*, 2000]. Knowledge of the optical constant (spectral complex refractive index) pertinent to each chemical compound and mixing structure is necessary for this process. Our knowledge is still limited due to uncertainties associated with optical constants [Haywood *et al.*, 2003; Bond and Bergstrom, 2004]; lack of reliable theory for modeling the mixture structure of optical constants of multicomponent aggregates [Sokolik and Toon, 1999]; and difficulties related to non-spherical particles [Mishchenko *et al.*, 2000].

[9] Model data used in this work are from the GOCART (Global Ozone Chemistry Aerosol Radiation and Transport) model developed by Georgia Institute of Technology and NASA GSFC. It is a three-dimensional chemical transport model with a horizontal resolution of  $2.5^\circ$  in longitude by  $2^\circ$  in latitude and 20–30 vertical layers [Chin *et al.*, 2000, 2002; Ginoux *et al.*, 2001]. In the model, emissions of key types of aerosols (sulfate, dust, organic carbon, black carbon and sea salt) and their precursors are estimated based on the state-of-the-art fossil/bio-fuel combustion; biomass burning; surface topographic features databases; the background meteorological condition is taken from Goddard Earth Observing System Data Assimilation System (GEOS DAS); the chemical reactions (DMS and  $\text{SO}_2$  oxidation *et al.*), transportation mechanisms (advection, diffusion and convection) and aging and removing processes (clustering, gravitational settling, wet deposition, washing-out *et al.*) are built in the model to simulate the aerosol evolution. The aerosol particle density, size distribution and complex refractive index were taken from Global Aerosol Data Set [Köepke *et al.*, 1997]. External mixing is used to composite various components into ambient aerosols.

## 2.2. Satellite Retrievals

[10] Over the last two decades, numerous satellite sensors have been designed to retrieve aerosol optical depths [King *et al.*, 1999]. Operational products have been obtained from Advanced Very High Resolution Radiometer (AVHRR) [Stowe *et al.*, 1997; Husar *et al.*, 1997; Higurashi and Nakajima, 1999; Mishchenko *et al.*, 1999; Ignatov and Stowe, 2002; Geogdzhayev *et al.*, 2002]; Total Ozone Mapping Spectrometer (TOMS)/Ozone Monitoring Instrument (OMI) [Herman *et al.*, 1997; Torres *et al.*, 1998, 2003]; Moderate Resolution Imaging Spectroradiometer (MODIS) [Kaufman *et al.*, 1997; Tanré *et al.*, 1997; Remer *et al.*, 2005], Multiangle Imaging Spectroradiometer (MISR) [Diner *et al.*, 1998; Martonchik *et al.*, 1998, 2004; Kahn *et al.*, 2005] and Polarization and Directionality of the Earth's Reflectance (POLDER) [Deuzé *et al.*, 2000, 2001]. Similar activity has been extended to other polar-orbiting sensors, such as SeaWiFS [Gordon and Wang, 1994], GLI [Nakajima *et al.*, 1998], OCTS [Nakajima *et al.*, 1999], ASTR-2 [Veeffkind *et al.*, 1999], VIRS [Ignatov and Stowe, 2000], MERIS [Ramon and Santer, 2001], ATSR [Holzer-Popp *et al.*, 2002], ETM+ [Lyapustin *et al.*, 2004], as well as to geostationary satellites, such as GOES-8 [Knapp *et al.*, 2002; Wang *et al.*, 2003a, 2003b]. In addition, several new instruments (CNES-PARASOL/POLDER, NASA/CNES-CALIPSO/CALIOP, EUMETSAT-MSG/SEVIRI, NOAA-NPOESS/VIIRS, NASA-GLORY/APS and NOAA-GOESR/ABI) have been or will be launched. Such enrichment of space platforms and

capabilities will open great opportunities to enhance our understanding and description of ambient aerosols.

[11] Other techniques (e.g., spaceborne lidar [Winker *et al.*, 2002; Léon *et al.*, 2003]) have been explored to augment satellite capabilities. Studies have been extended to derive other fundamental parameters (e.g., single scattering albedo [Kaufman *et al.*, 2001; Torres *et al.*, 2005; Chowdhary *et al.*, 2005; Satheesh and Srinivasan, 2005]; size distribution and real refractive index [Deuzé *et al.*, 2000, 2001; Chowdhary *et al.*, 2002]). Consequently, remote sensing from space plays a key role in aerosol research.

[12] In this work, aerosol information from space-borne measurements is taken from the MODIS Collection 4 product. MODIS is well designed for aerosol retrievals [Salomonson *et al.*, 1989]. With thirty-six well-calibrated bands, a wide spectral range (from visible to infrared) of radiance observations provided is the stage for implementing more accurate cloud screening algorithms and for determining the surface reflectance across the solar spectrum. Also benefiting from fine spatial resolution and near daily global coverage, MODIS presents an unprecedented chance to monitor global aerosol characteristics with a relatively high accuracy. Detailed attention was given to calibration, cloud screening, surface effects and assumptions on aerosol properties.

## 2.3. Aeronet Ground Observations

[13] AERONET [Holben *et al.*, 1998] is a globally distributed federated network of ground-based observations representing a wide variety of atmospheric conditions. AERONET imposes standardization on measurement protocol, data processing and calibration, and uses the weather-resistant automatic CIMEL sun-sky radiometer, which enable frequent measurements of atmospheric aerosol optical properties at remote sites. Estimates of aerosol intensive parameters, microphysical (size distribution) and optical constants (complex reflective index) are based on optimal statistical analysis [Dubovik and King, 2000]. Sky-radiances at multispectra (0.44, 0.67, 0.87, and  $1.02 \mu\text{m}$ ) and multi-angles combined with estimated AOD and various a priori constraints serve as multisource data with predetermined accuracy. Search for best fit is carried out by maximum likelihood method. Success of retrievals demands homogeneous clear-sky conditions (radiances from at least 21 out of 27 scattering angles are symmetric on both sides of the Sun), high aerosol loadings ( $\tau_{0.44, \mu\text{m}} > 0.4$ ) and large solar zenith angles ( $\geq 45^\circ$ ). Given the infrequency of sky radiance measurements (made at optical air masses of 4, 3, and 2 in the morning and afternoon, and once per hour in-between) and strict quality requirements, the number of retrievals is limited.

## 3. Methodology

### 3.1. Aerosol Single Scattering Albedo

[14] The direct radiative effect of aerosols is sensitive to the single scattering albedo ( $\omega_0$ ) [Hansen *et al.*, 1997; Satheesh and Ramanathan, 2000]; however, observations of aerosol absorbing properties are limited and difficult to obtain [IPCC, 2001]. At present, no reliable global column aerosol SSA data sets from satellite retrievals are available. In this study, characterization of the single scattering albedo

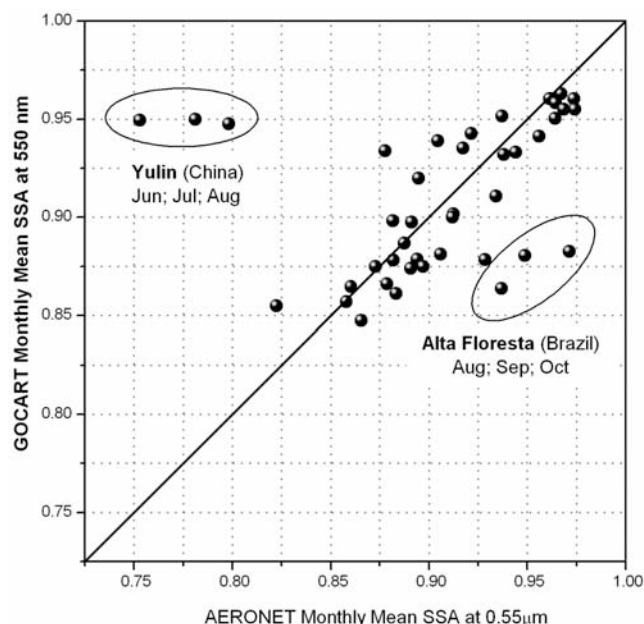


**Figure 2.** Scatterplot of GOCART monthly mean SSA at 550 nm against AERONET almucantar retrievals for the year 2001. Monthly mean AERONET SSA is calculated if more than five days data are available. Outliers are basically associated with two stations (Yulin and Alta Floresta) in the boreal summer and autumn time.

is based on GOCART model result and AERONET almucantar retrievals.

### 3.1.1. Gocart Model Simulated Global SSA at 0.55 $\mu\text{m}$

[15] Column aerosol SSA can be calculated from the simulated concentration of each aerosol component, assumed complex refractive index and particle size and shape. GOCART model incorporates five key components (sulfate, dust, organic carbon, black carbon and sea salt). Particle density, size distribution and complex refractive index were taken from Global Aerosol Data Set (GADS) with dependence on ambient relative humidity [Köepke *et al.*, 1997]. Homogeneous spherical and external mixtures are assumed to calculate aerosol column SSA.

[16] A scatterplot of GOCART monthly mean SSA for year of 2001 against available AERONET almucantar retrievals is presented in Figure 2. We have interpolated the AERONET values at 0.55  $\mu\text{m}$  from 0.44 and 0.67  $\mu\text{m}$  data if more than five retrievals are available within one month. Majority of GOCART simulated  $\omega_0$  (76%, 32 out of 42 pairs) fall within the uncertainty of AERONET retrievals ( $\pm 0.03$ ); however, outliers do exist with the most obvious ones coming from two stations (Yulin, China and Alta Floresta, Brazil) at boreal summer and autumn time. It is difficult to ascertain if such large discrepancies are due to model deficiencies or sampling issues. An effort has been made to examine the quality of GOCART aerosol intensive properties, yet it is still in a preliminary stage due to scarcity of high quality measurements [Chin, private communication]. Therefore corrections based on AERONET observations are not attempted here and aerosol  $\omega_0$  at 0.55  $\mu\text{m}$  from GOCART model is accepted “as is” (when additional large scale information on  $\omega_0$  will become available, it will be merged with what is used now).

### 3.1.2. Spectral Variation of Aerosol SSA From Aeronet Retrievals

[17] Chemical composition and microphysical properties determine the spectral variation of aerosol  $\omega_0$ . Measurements reveal two types of wavelength dependencies for absorbing aerosols: decreasing  $\omega_0$  as a function of wavelength, associated with small-sized aerosols that contain black and organic carbon [Bergstrom *et al.*, 2002, 2003; Kirchstetter *et al.*, 2004; Dubovik *et al.*, 1998, 2002a]; and increasing  $\omega_0$  as a function of wavelength, associated with dust dominated aerosols [Sokolik and Toon, 1999; Dubovik *et al.*, 2002a; Bergstrom *et al.*, 2004; Torres *et al.*, 2005; Eck *et al.*, 2005]. In the first case the variation is largely due to the stronger decrease of the scattering coefficient with wavelength as compared to the absorption coefficient; in the second case, it is mainly attributed to the larger imaginary refractive index of mineral dust at the short end of the solar spectrum [Patterson *et al.*, 1977; Alfaro *et al.*, 2004]. Consequently, analysis of spectral variations of  $\omega_0$  is executed separately for dust and other aerosols as described in what follows.

[18] More than ten years (1993 to 2003) of instantaneous AERONET almucantar retrievals are used to demonstrate and analyze the spectral variations of  $\omega_0$ . They are grouped by their value at 0.55  $\mu\text{m}$  at 0.01 bin intervals. For dust dominated conditions, results based on spheroid assumption retrievals are used due to their superior quality compared to spherical assumption [Dubovik *et al.*, 2002b]. Figure 3 shows the spectral variation as a functions of aerosol type (dust versus non-dust) and of  $\omega_0$  at 0.55  $\mu\text{m}$ . There is indication that the single-scattering albedo spectral slope can be generally steeper for pollution aerosols [Bond and Bergstrom, 2006] than for biomass burning [Reid *et al.*, 2005]. In this study pollution aerosols were not separated from smoke.

### 3.1.3. Monthly Mean Aerosol SSA Over the Solar Spectrum

[19] To apply the newly derived spectral variations (Figure 3) to GOCART  $\omega_0$  at 0.55  $\mu\text{m}$  requires the identification of aerosol type (dust or non-dust). We use MODIS derived monthly mean Ångström exponent ( $\alpha$ ) combined with merged  $\tau_{0.55\mu\text{m}}$  [Liu *et al.*, 2005] to specify regions where dust aerosol dominates. It should be noted that Ångström exponent and AOT must be used with caution in identifying mineral dust. For example, Kaufman *et al.* [2005] suggested an empirical scheme to account for the size overlap among different aerosol types when seeking to separate mineral dust from spherical particles. Distinction between spherical and non-spherical particles can be based on the MISR multiangle data [Kalashnikova and Kahn, 2006] (information not available at the time of this study).

[20] Over bright surfaces no retrievals are made from MODIS observations; therefore, we perform data-filling as follows: 1) for high latitudes ( $>60^\circ$ ), we replace missing values with data from nearest available month; otherwise, latitudinal average is used; 2) linear interpolations in space are performed to fill in the remaining voids. Since MODIS provides  $\alpha_{0.44-0.66\mu\text{m}}$  over land and  $\alpha_{0.55-0.87\mu\text{m}}$  and  $\alpha_{0.87-2.13\mu\text{m}}$  over ocean, a second order polynomial fit is used to estimate  $\alpha_{0.44-0.66\mu\text{m}}$ . Dust aerosols are determined by the criteria that over land  $\alpha_{0.44-0.66\mu\text{m}}$  is less than 0.75 (same threshold was used by Eck *et al.* [2005], but

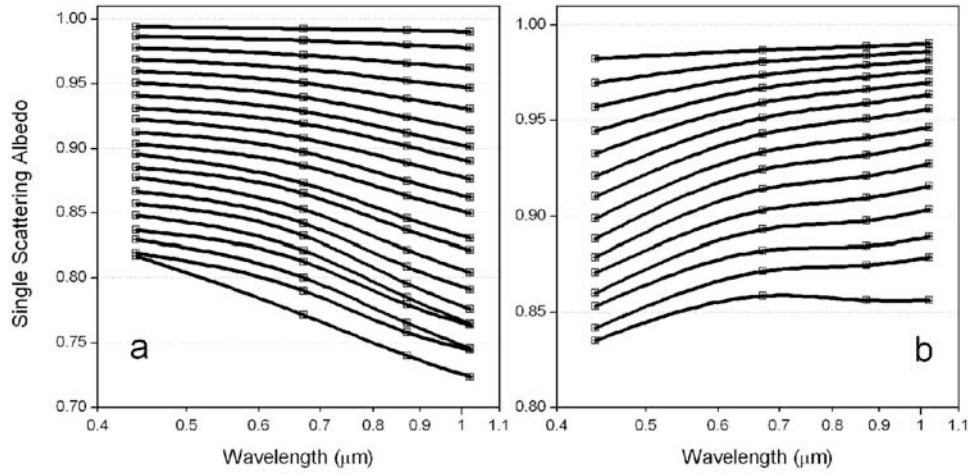


**Figure 3.** Spectral variation of aerosol single scattering albedo derived in this study from more than 6000 instantaneous AERONET almucantar retrievals from 1993 to 2003. Data are binned at 0.01 intervals of  $\omega_0$  at  $0.55 \mu\text{m}$  (a) fine mode dominant; (b) coarse mode dominant (dust).

applied to  $\alpha_{0.44-0.87\mu\text{m}}$ ); over ocean an additional requirement of  $\tau_{0.55\mu\text{m}}$  larger than 0.2 is enforced to separate from large sea salt particles (relatively low optical depth of maritime aerosols). Figure 4 displays the successfully identified major dust source regions (North Africa, Middle East, Central Asia, China as identified by *Prospero et al.* [2002]; and Australia, part of America and South Africa) and transports areas (tropical Atlantic and Northern Pacific). Having such information on aerosol type and the GOCART model  $\omega_0$  at  $0.55 \mu\text{m}$ , the appropriate wavelength dependent curve can be selected from Figure 3. Expansion of  $\omega_0$  to the whole solar spectrum is performed based on linear interpolation/extrapolation with respect to the logarithm of wavelength.

### 3.2. Aerosol Asymmetry Parameter

[21] Aerosol asymmetry parameter ( $g$ ) is primarily determined by particle shape, size distribution and real part of the refractive index. Background of Figure 5 shows the variation of  $g$  as functions of particle size and real refractive index based on theoretical analysis [*Hansen and Travis*, 1974]. In terms of geometric optics, local maxima and minima can be interpreted as the result of interference of light diffracted and transmitted by the particle. For the majority of ambient aerosols, real part of refractive index varies around the value of 1.5 within a limited range ( $\pm 0.15$ ) [*Köepke et al.*, 1997]; therefore, given the widely adopted spherical shape assumption, size distribution might be the governing factor affecting the spectral variation of  $g$ . In this work, we obtain a global description of  $g$  from the size information inferred from MODIS remote sensing product.

#### 3.2.1. Relationship Between Asymmetry Parameter and Ångström Exponent

[22] Ångström exponent ( $\alpha$ ), a fundamental product from multispectral satellite retrievals (e.g., from MODIS, MISR, two-channel AVHRR), provides information about aerosol size. Theoretical studies revealed that  $\alpha$  can be related to the Junge (power law) number size distribution [*Junge*, 1955]:

$$\frac{dN}{d \ln r} = cr^{-\nu} \quad (1)$$

by  $\alpha = \nu - 2$  [*Van de Hulst*, 1957; *Bullrich*, 1964]. A more frequently used statement is an inverse relationship between  $\alpha$  and particle size, namely, the larger the exponent, the smaller the particles. Because of theoretical difficulties (e.g., interpreting  $\alpha$  for multimodal aerosol distributions and the nonspherical particle shape) and large variations associated with aerosol size distribution, this relationship has not been explored beyond its use as a qualitative indicator.

[23] To develop a relationship between  $\alpha$  and  $g$ , we produce a scatterplot of asymmetry parameters versus effective size parameters estimated from  $\alpha_{0.44-0.67\mu\text{m}}$  (Figure 5). Data used are the instantaneous AERONET almucantar retrievals at 4 wavelengths ( $0.44$ ,  $0.67$ ,  $0.87$ , and  $1.02 \mu\text{m}$ ) from 1993 to 2003; we require  $\tau_{0.44\mu\text{m}} > 0.3$  due to the higher retrieval quality for the higher loading cases. There is a similarity in magnitude and variability when compared with theoretical studies. We fit the scatter points by a regression analysis of a two-step Gaussian curve:

$$g_\lambda = \begin{cases} a_2 \exp\left(-\frac{(x-a_0)^2}{2a_1^2}\right) & \text{when } \ln x < 1.9 \\ b_3 - b_2 \exp\left(-\frac{(x-b_0)^2}{2b_1^2}\right) & \text{when } \ln x \geq 1.9 \end{cases} \quad (2)$$

Values of corresponding coefficients are presented in Table 1. The independent variable is the approximated effective size parameter  $x$  derived from  $\alpha_{0.44-0.67\mu\text{m}}$  by:

$$x = 0.8\pi / \lambda \alpha_{0.44-0.67\mu\text{m}} \quad (3)$$

#### 3.2.2. Global Monthly Mean Asymmetry Parameter Over the Solar Spectrum

[24] Using the empirical relationship of equation (2), we estimate the global monthly averaged aerosol asymmetry parameter as a function of wavelength using MODIS  $\alpha_{0.44-0.66\mu\text{m}}$  (derived from  $\alpha_{0.55-0.87\mu\text{m}}$  and  $\alpha_{0.87-2.13\mu\text{m}}$  over ocean based on a second order polynomial fit) for year 2001 (Figure not shown). Small values of  $g_{0.55\mu\text{m}}$  ( $< 0.6$ ) are associated with regions dominated by urban pollution (e.g.,

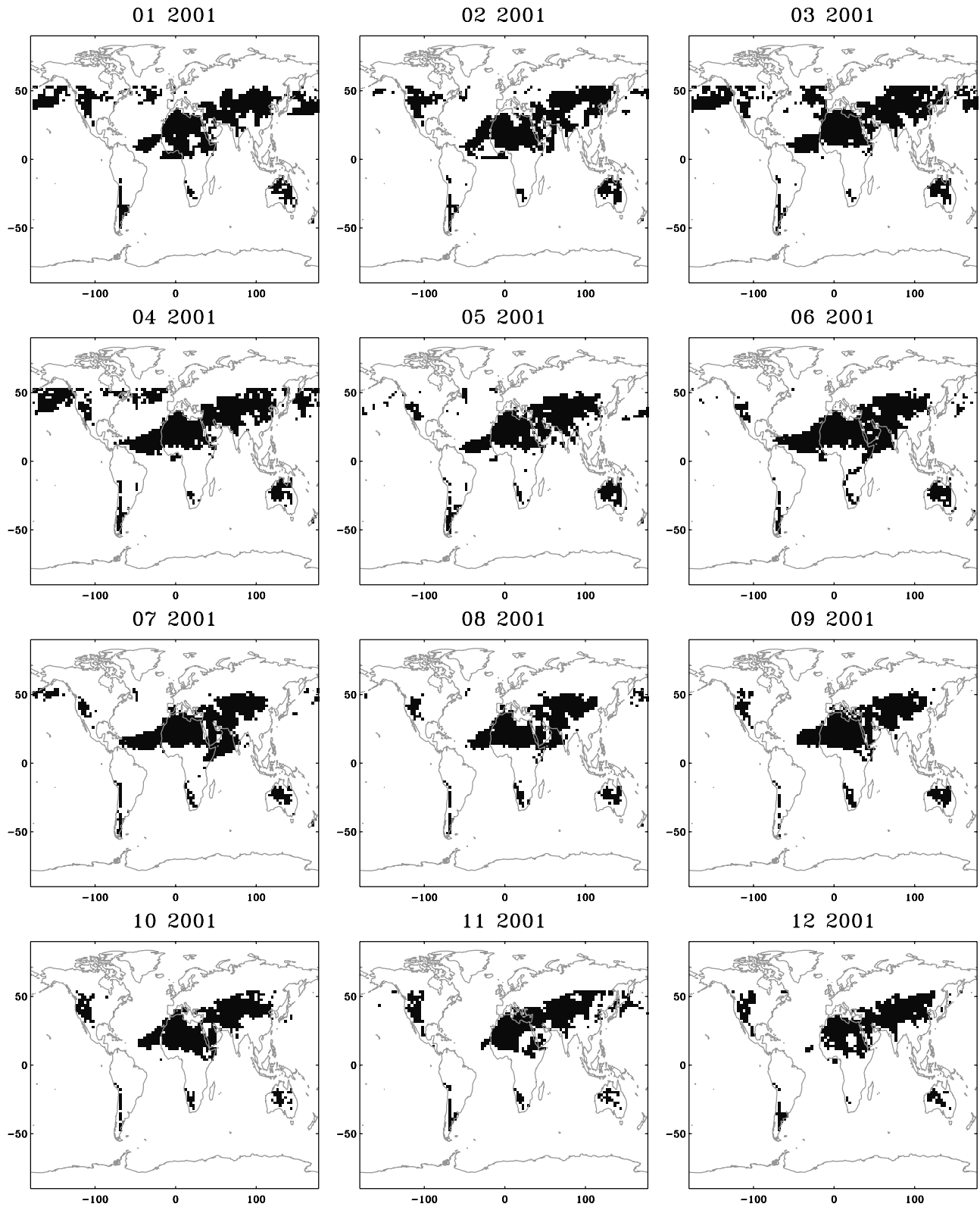


**Figure 4.** Dust dominated areas identified on the basis of MODIS  $\alpha_{0.44-0.87\mu\text{m}}$  and merged  $\tau_{0.55\mu\text{m}}$ .

East US and Europe) and biomass burning (e.g., South America, South Africa and Southeast Asia); while the larger  $g_{0.55\mu\text{m}}$  ( $> 0.7$ ) are present over oceans (sea salt particles). Dust over North Africa, Middle East and Central Asia has

values between 0.65 and 0.7. Compared to Reported is a median value of 0.7 from measurements at coastal areas and ocean sites [Hartley and Hobbs, 2001; Eck et al., 2001], approximate value of 0.54 for biomass burning in Brazil

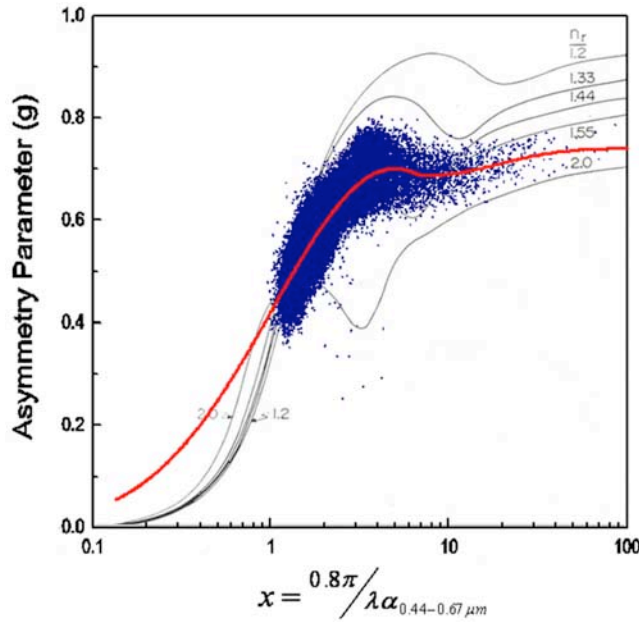


**Figure 5.** Background: Asymmetry parameter  $\langle \cos \alpha \rangle$  ( $g$ ), as a function of effective size parameter ( $x = 2 \pi a / \lambda$ ). Results are shown for five values of the real refractive index,  $n_r$ , all with  $n_i = 0$ . A variation of gamma size distribution was used with effective variance  $b = 0.07$  [Hansen and Travis, 1974, Figure 12]. Superimposed: Scatterplot of asymmetry parameter against approximate effective size parameter ( $x = 0.8 \pi / \lambda \alpha_{0.44-0.67 \mu m}$ ) from instantaneous AERONET almucantar retrievals ( $\tau_{0.44 \mu m} > 0.3$ ) at 4 wavelengths (0.44, 0.67, 0.87, and 1.02  $\mu m$ ). Gray curve is the regressed empirical relationships.

[Ross *et al.*, 1998], and an average value of 0.68 for dust aerosols [Dubovik *et al.*, 2002a], in good agreement with our estimates.

[25] Limitations associated with this parameterization scheme are:

[26] 1). Qualitative understanding of the inverse relationship between effective particle size ( $r_{eff}$ ) and Ångström exponent ( $\alpha_{0.44-0.67 \mu m}$ ) is based on the assumption that:

$$r_{eff} = 0.4 / \alpha_{0.44-0.67 \mu m} \quad (4)$$

Support for this assumption is provided by Figure 6 in which we show the histogram of  $r_{eff} * \alpha_{0.44-0.67 \mu m}$  for more than 58,200 AERONET instantaneous retrievals from 1993 to 2003. A single peak exists around the value 0.4. However, problems arise from cases included in the extended tails. Furthermore, presence of negative  $\alpha$

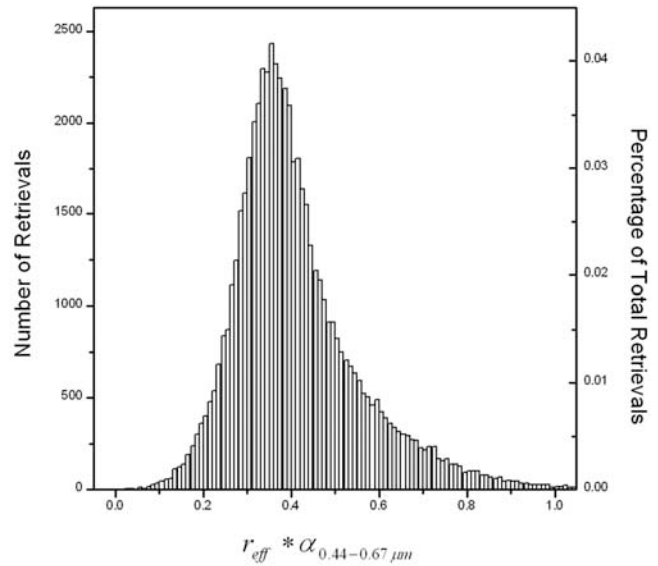


**Figure 6.** Histogram of  $r_{eff} * \alpha_{0.44-0.67 \mu m}$ , derived from more than 58,200 available AERONET instantaneous almucantar retrievals from 1993 to 2003.

invalidates assumption of equation (4) and requires special attention (in applications a negative  $\alpha_{0.44-0.67 \mu m}$  is changed to 0.01).

[27] 2). The empirical relationship represents average conditions, and therefore, is unable to capture the detailed variations displayed in Figure 5.

[28] 3). Concern about the applicability of the empirical relationship to fine mode dominated aerosols at longer wavelengths ( $>1.02 \mu m$ ). As seen in Figure 5, this is the domain where data from AERONET retrievals are not available ( $x < 1$ ). We base the projected monotonic decrease of  $g$  with the decrease of  $x$  on the theoretical relationship presented in the background of Figure 5. Such variation is based on simulations with a variation of gamma size distribution (characterized by a single mode as used by Hansen and Travis [1974]), which might miss the influence of coarse mode particles. Figure 7 illustrates the effect of the coarse mode particles on  $g$  as a function of wavelength and effective size parameter for the Goddard Space Flight Center (GSFC) urban aerosol model [Dubovik *et al.*, 2002a]. Incorporation of coarse mode greatly changes the variation trend of  $g$  in a region where  $x < 1.5$  (or  $\lambda > 1 \mu m$ ). This can be explained by the increased influence of large particles and reduced scattering contribution from the fine mode when a “small particle regime” is approached. Therefore even an insignificant amount of coarse mode particles could dominate the behavior of  $g$  in this region. Coexistence of fine and coarse mode particles in ambient aerosols is quite common as discussed in several studies [Whitby, 1978; Shettle and Fenn, 1979; Remer and Kaufman, 1998; Dubovik *et al.*, 2002a]. Accuracy of the MODIS derived  $\alpha$  will also affect the quality of the derived  $g$ . Evaluation of instantaneous MODIS retrieved  $\alpha_{0.44-0.67 \mu m}$  over land revealed differences when compared with AERONET measurements [Chu *et al.*, 2002].

**Table 1.** Coefficients of the Empirical Relationship (Equation (2)) Used to Derive Asymmetry Parameter From Ångström Exponent

$a_0$	$a_1$	$a_2$	
1.61379	1.59757	0.69420	
$b_0$	$b_1$	$b_2$	$b_3$
2.08552	0.84890	0.05382	0.742232

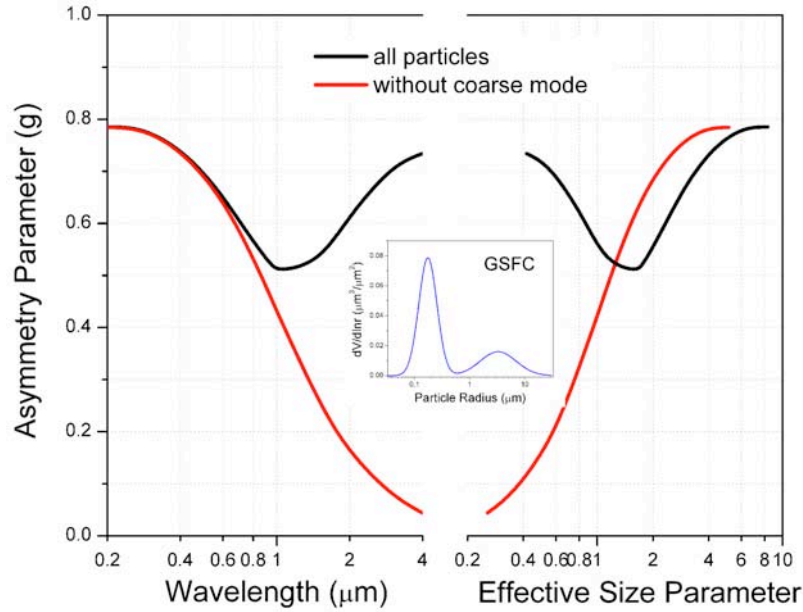


**Figure 7.** Effect of coarse mode particles on asymmetry parameter as functions of wavelength and effective size parameter. Inner panel is the volume size distribution of aerosols at GSFC [Dubovik *et al.*, 2002a] where a Bi-modal lognormal function is used:  $\frac{dV}{d \ln r} = \sum_{i=1}^2 \frac{C_{v,i}}{\sqrt{2\pi}\sigma_i} \exp\left(-\frac{(\ln r - \ln r_{v,i})^2}{2\sigma_i^2}\right)$  Parameters were calculated for the case where  $\tau_{0.44\mu\text{m}} = 0.5$ , which leads to: 1) fine mode:  $R_{v,1} = 0.175\mu\text{m}$ ,  $\sigma_1^2 = 0.144$ ,  $C_{v,1} = 0.075$ ; 2) coarse mode:  $R_{v,2} = 3.275\mu\text{m}$ ,  $\sigma_2^2 = 0.563$ ,  $C_{v,2} = 0.030$ .

### 3.3. Aerosol Normalized Extinction Coefficient

[29] Spectral variation of  $\alpha$  has been reported previously [Eck *et al.*, 1999; O'Neill *et al.*, 2001]. Since over land, MODIS retrievals are made only in two channels, in our calculations we assume a wavelength independent  $\alpha$  ( $=\alpha_{0.44-0.66\mu\text{m}}$ ) of the normalized extinction coefficients between 0.2 to 4.0  $\mu\text{m}$ . Over oceans, we use a second order polynomial fit to  $\ln \tau$  versus  $\ln \lambda$  (based on  $\alpha_{0.55-0.87\mu\text{m}}$  and

$\alpha_{0.87-2.13\mu\text{m}}$ ) to estimate the spectral variation of aerosol extinction.

### 4. Sensitivity Tests

[30] Due to the lack of reliable measurements at large scale, global characterization of aerosol optical properties is subject to uncertainties. Simulations are performed to eval-

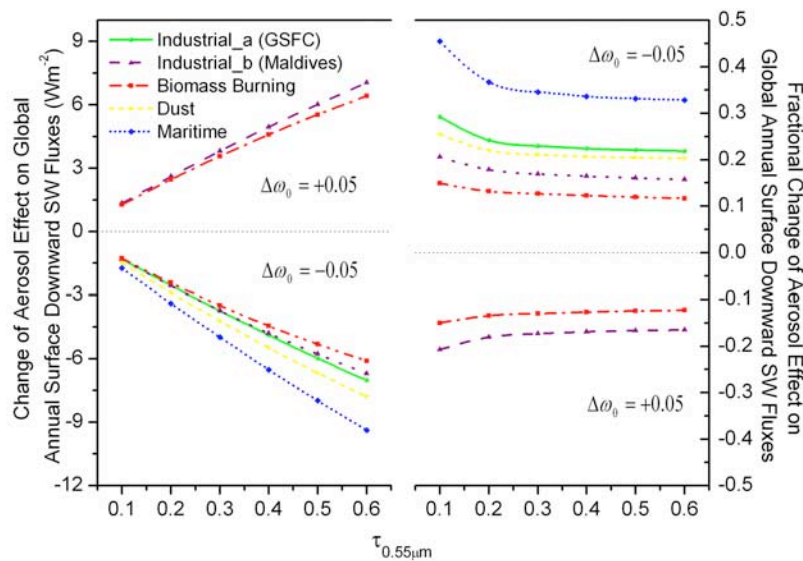


**Figure 8.** Changes of global annually averaged aerosol direct effects on the surface downward SW fluxes for various types of aerosols due to  $\pm 0.05$  uncertainty of  $\omega_0$ . Cases where increase of 0.05 results in  $\omega_0$  being beyond 1.0 are not simulated (GSFC, Dust and Maritime aerosols). Left Panel: change of flux values ( $\text{Wm}^{-2}$ ); Right panel: fractional changes (the ratio of the change and original surface effect).

**Table 2.** Changes of Backscattered Fraction for Isotropically Incident Radiation ( $\bar{\beta}$ ) Due to  $\pm 0.1$  Variations of  $g$  for Various Types of Aerosols

Aerosol Type	$g$ (SW broadband Average)	$\Delta g = +0.1$		$\Delta g = -0.1$	
		$\Delta \bar{\beta}$	$\Delta \bar{\beta}/\bar{\beta}$	$\Delta \bar{\beta}$	$\Delta \bar{\beta}/\bar{\beta}$
Industrial (a)	0.677821	-0.051448	-0.22902	0.046427	0.20667
Industrial (b)	0.688620	-0.052154	-0.23774	0.046865	0.21363
Biomass burning	0.607242	-0.047670	-0.18490	0.043998	0.17066
Dust	0.661138	-0.050433	-0.21675	0.045788	0.19679
Maritime	0.778430	-0.060243	-0.34850	0.051486	0.29785

uate the sensitivity of aerosol surface effects on the inaccurate knowledge of aerosol single scattering albedo and asymmetry parameters.

[31] Following the methodology used for estimation of aerosol TOA radiative forcing [Charlson *et al.*, 1991, 1992; Penner *et al.*, 1992; Chylek and Wong, 1995; Hobbs *et al.*, 1997], radiative transfer calculations are performed with an aerosol layer inserted between the aerosol-free atmosphere and the surface. Global annual averaged reduction of surface insolation is calculated as follows:

$$\overline{\Delta SWF_{surf}} = \frac{1}{4} S_0 (1 - \bar{A}_c) \Delta F_{surf} \quad (5)$$

where  $\frac{1}{4} S_0$  is the global average of incoming solar radiation ( $343 \text{ Wm}^{-2}$ ) and  $\bar{A}_c$  is the global average fraction of cloud cover (60%). Aerosol-induced change of the normalized surface SW downward flux ( $\Delta F_{surf}$ ) can be represented as:

$$\Delta F_{surf} = \frac{T_{tot}}{1 - R_{tot}^\uparrow \alpha} - \frac{T_{atm}}{1 - R_{atm} \alpha} \quad (6)$$

where  $T_{tot}$  is the total columnar transmittance and  $R_{tot}^\uparrow$  is the combined (atmosphere and aerosol layers) reflectance for the bottom illumination. The average spherical transmittance and reflectance of the Rayleigh sky above the aerosol layer is  $T_{atm}$  and  $R_{atm}$  and for the aerosol layer it is  $T_{aer}$  and

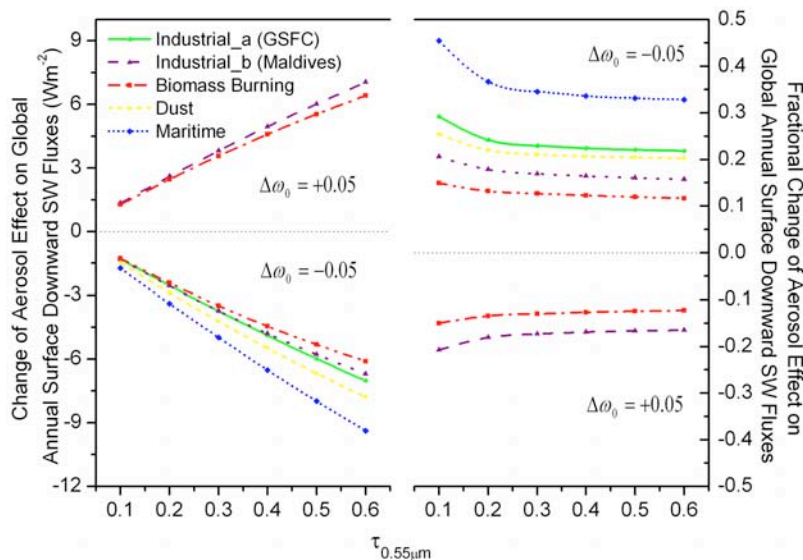
$R_{aer}$ .  $\alpha$  is the underlying surface albedo. The adding equation [Hansen and Travis, 1974] for the combined atmosphere and aerosol column will yield:

$$T_{tot} = T_{atm} T_{aer} / (1 - R_{atm} R_{aer}) \quad (7)$$

$$R_{tot}^\uparrow = R_{aer} + R_{atm} T_{aer}^2 / (1 - R_{atm} R_{aer}) \quad (8)$$

For a clear-sky aerosol-free atmospheric layer, the values of optical functions ( $R_{atm}$  and  $T_{atm}$ ) are taken from a global average, namely,  $R_{atm} = 0.06$ ,  $T_{atm} = 0.77$  (with about 4% and 13% solar radiation being absorbed by  $O_3$  and water vapor), and global averaged surface albedo of 0.15 is assumed [Charlson *et al.*, 1992]. For the aerosol layer two-stream formulations are used to estimate  $T_{aer}$  and  $R_{aer}$  [Coakley and Chylek, 1975]. Simulations are carried out for urban (two types: a. from GSFC; b. from Maldives), biomass burning, dust and maritime aerosols [Dubovik *et al.*, 2002a] with  $\tau_{0.55\mu m}$  varying from 0.1 to 0.6.

[32] Figure 8 shows the changes of global annually averaged aerosol direct effect due to  $\pm 0.05$  uncertainty in aerosol single scattering albedo. Increasing aerosol absorption ( $\Delta \omega_0$ ) leads to a further depletion of surface SW radiation; the most significant effect is associated with the least absorbing aerosols (sea salt). Sensitivity is also depen-

**Figure 9.** Changes of the global annually averaged aerosol direct effects on the surface downward SW fluxes for various types of aerosols due to  $\pm 0.1$  uncertainty of  $g$ . Left Panel: change of flux values ( $\text{Wm}^{-2}$ ); Right panel: fractional changes.

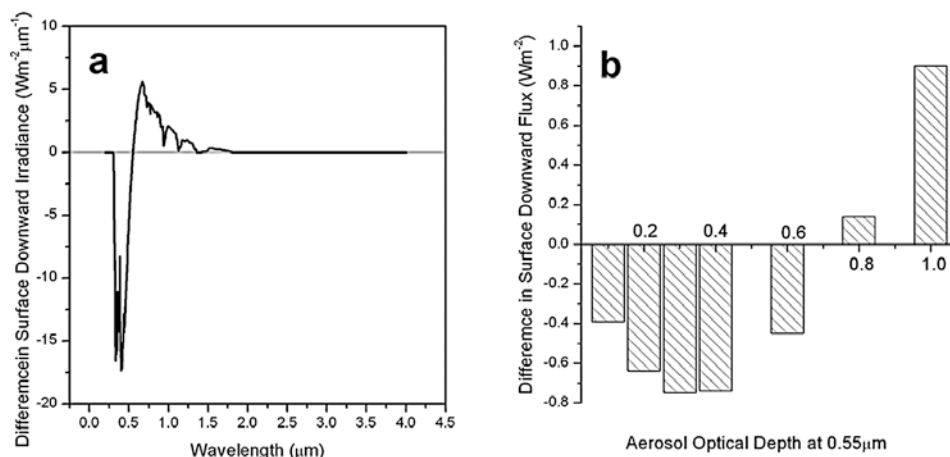


**Figure 10.** Comparison of simulation results using spectrally resolved aerosol  $\omega_0$  and  $g$  versus assumed mid-visible ( $0.55 \mu\text{m}$ ) value for the entire solar spectrum. GSFC urban aerosol and vegetation surface was used in the simulation. Solar zenith angle was set to 45 degree. Displayed are difference (spectrally uniform minus resolved) in (a) surface downward irradiance over solar spectrum at aerosol optical depth at  $0.55 \mu\text{m}$  of 0.2; and (b) surface downward shortwave flux as a function of aerosol optical depth at  $0.55 \mu\text{m}$ .

dent on the aerosol asymmetry parameter ( $g$ ) with stronger effects related to the more powerful forward scattering particles (larger  $g$ ), as seen for dust and for GSFC aerosols that have similar  $\omega_0$ . Assuming that the global average  $\tau_{0.55\mu\text{m}}$  is 0.15, a 0.05 uncertainty in  $\omega_0$  would translate to an averaged error of about  $2 \text{ Wm}^{-2}$  (20%) on the global annual averaged aerosol direct surface effect.

[33] Sensitivity tests are also carried out to assess the influence of  $\pm 0.1$  variations of  $g$  for various types of aerosols on the global annual surface irradiance. Table 2 shows that influence on the backscattered fraction  $\beta$  is dependent on the actual value of  $g$ : the higher the asymmetry parameter the larger is the effect. In terms of impact on the surface downward SW fluxes, such dependence is further strengthened by the positive correlation between  $g$  and  $\omega_0$  as revealed in Figure 1 (higher  $\omega_0$  indicates a larger part of extinction is affected by the uncertainty of  $g$ ). Figure 9 illustrates variation of effects associated with different types of aerosols. Assuming a globally averaged  $\tau_{0.55\mu\text{m}}$  of 0.15, a 0.1 uncertainty in  $g$  would result in an

influence from 1 to  $2 \text{ Wm}^{-2}$  on the aerosol direct effects on surface irradiance.

[34] Sensitivity tests to evaluate the difference in surface downward shortwave fluxes using spectrally resolved aerosol  $\omega_0$  and  $g$  versus assumed mid-visible ( $0.55 \mu\text{m}$ ) value for the entire solar spectrum, have been performed. In Case # 1 used is the GSFC urban aerosol model of *Dubovik et al.* [2002a]. In Figure 10 shown is the total difference in the surface downward shortwave flux as a function of aerosol optical depth, once for spectrally resolved case and once assuming the mid-visible ( $0.55 \mu\text{m}$ ) value for the entire solar region. As evident, using the mid-visible values of SSA and  $G$  will introduce less than  $1 \text{ W/m}^2$  for the total SW flux but there will be a difference of more than  $10 \text{ W/m}^2/\mu\text{m}$  for aerosol optical depth of 0.2 in the UV and visible. In Case # 2 used is the Biomass burning (Zambia in South Africa) from *Dubovik et al.* [2002a]. As evident from Figure 11, using the mid-visible values of  $\omega_0$  and  $g$  will introduce over  $8 \text{ W/m}^2$  for the total SW flux for optical depth larger than 0.8 and significant difference (more than

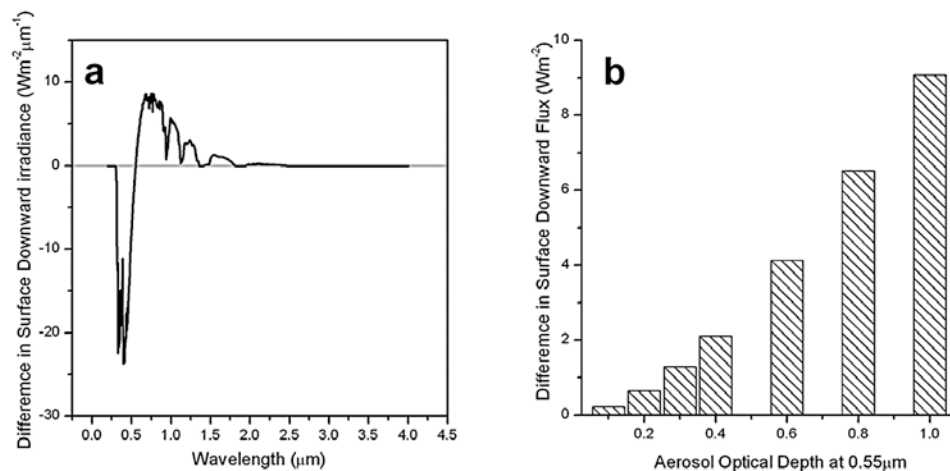


**Figure 11.** Similar to Figure 10, but for biomass burning aerosol from South Africa.

10 W/m<sup>2</sup>/μm at aerosol optical depth of 0.2) in the UV and visible.

## 5. Summary

[35] In this study, we estimate monthly mean aerosol optical properties in the SW spectrum at global scale, based on GOCART model simulations, MODIS retrievals and AERONET measurements/retrievals. The single scattering albedo is obtained by extending GOCART  $\omega_0$  at 0.55 μm to the entire SW spectrum using spectral dependence derived from available AERONET retrievals. The asymmetry parameters over the solar spectrum are determined from MODIS Ångström wavelength exponent, utilizing an empirical relationship derived from AERONET almucantar retrievals. The normalized extinction coefficient is estimated from the MODIS Ångström wavelength exponents. At present, information on aerosol AOD is readily available from space. Information on aerosol single scattering albedo comes from model simulations. More recent space observations from TOMS, OMI, MISR, and from planned satellite sensors (e.g., Aerosol Polarimetry Sensor) focus on the absorbing properties of aerosols. Sensitivity tests were performed for  $\omega_0$  and  $g$  to assess effects on surface downward SW fluxes. For an assumed global average  $\tau_{0.55 \mu m}$  of 0.15, a perturbation of 0.05 and 0.1 in  $\omega_0$  and  $g$  will result in about 2.0 and 1.5 Wm<sup>-2</sup> flux change, respectively. The work presented here provides a realistic framework for merging data from independent sources to generated needed information on aerosols.

[36] **Acknowledgments.** Support by the NASA Earth System Science Fellowship grant NGT530450 and NASA EOD/IDS grant NAG59634 to the University of Maryland is greatly appreciated. We are thankful to Ralph A. Kahn for the very insightful and helpful comments.

## References

- Alfaro, S. C., S. Lafon, J. L. Rajot, P. Formenti, A. Gaudichet, and M. Maille (2004), Iron oxides and light absorption by pure desert dust: An experimental study, *J. Geophys. Res.*, **109**, D08208, doi:10.1029/2003JD004374.
- Bergstrom, R. W., P. B. Russell, and P. Hignett (2002), Wavelength dependence of the absorption of black carbon particles: Predictions and results from the TARFOX experiment and implications for the aerosol single scattering albedo, *J. Atmos. Sci.*, **59**, 567–577.
- Bergstrom, R. W., P. Pilewskie, B. Schmid, and P. B. Russell (2003), Estimates of the spectral aerosol single scattering albedo and aerosol radiative effects during SAFARI 2000, *J. Geophys. Res.*, **108**(D13), 8474, doi:10.1029/2002JD002435.
- Bergstrom, R. W., P. Pilewskie, J. Pommier, M. Rabbette, P. B. Russell, B. Schmid, J. Redemann, A. Higurashi, T. Nakajima, and P. K. Quinn (2004), Spectral absorption of solar radiation by aerosols during ACE-Asia, *J. Geophys. Res.*, **109**, D19S15, doi:10.1029/2003JD004467.
- Bond, T. C., and R. W. Bergstrom (2004), Toward resolution on the optics of light-absorbing carbon. *AGU Fall Meeting*, Dec. 13–17, San Francisco, CA.
- Bond, T. C., and R. W. Bergstrom (2006), Light absorption by carbonaceous particles: An investigative review, *Aerosol Sci. Technol.*, **40**, 27–67.
- Boucher, O., and T. L. Anderson (1995), GCM assessment of the sensitivity of direct climate forcing by anthropogenic sulfate aerosols to aerosol size and chemistry, *J. Geophys. Res.*, **100**, 26,117–26,134.
- Bullrich, K. (1964), Scattered radiation in the atmosphere and the natural aerosol, *Advances in Geophysics*, **10**, Academic Press, 99–260.
- Bush, B. C., and F. P. J. Valero (2003), Surface aerosol radiative forcing at Gosan during the ACE-Asia campaign, *J. Geophys. Res.*, **108**(D23), 8660, doi:10.1029/2002JD003233.
- Charlson, R. J., J. Langner, H. Rodhe, C. B. Leovy, and S. G. Warren (1991), Perturbation of the Northern Hemisphere radiative balance by backscattering from anthropogenic sulfate aerosols, *Tellus, Ser. A and Ser. B*, **43A**, 152–163.
- Charlson, R. J., S. E. Schwartz, J. M. Hales, R. D. Cess, J. A. Coakley Jr., J. E. Hansen, and D. J. Hofmann (1992), Climate forcing by anthropogenic aerosols, *Science*, **255**, 423–430.
- Chin, M., R. B. Rood, S.-J. Lin, J.-F. Muller, and A. M. Thompson (2000), Atmospheric sulfur cycle simulated in the global model GOCART: Model description and global properties, *J. Geophys. Res.*, **105**, 24,671–24,687.
- Chin, M., P. Ginoux, S. Kinne, O. Torres, B. Holben, B. N. Duncan, R. V. Martin, J. A. Logan, A. Higurashi, and T. Nakajima (2002), Aerosol distributions and radiative properties simulated in the GOCART model and comparisons with observations, *J. Atmos. Sci.*, **59**, 461–483.
- Chowdhary, J., B. Cairns, and L. D. Travis (2002), Case studies of aerosol retrievals over the ocean from multiangle, multispectral photopolarimetric remote sensing data, *J. Atmos. Sci.*, **59**, 383–397.
- Chowdhary, J., B. Cairns, M. I. Mishchenko, P. V. Hobbs, G. F. Cota, J. Redemann, K. Rutledge, B. N. Holben, and E. Russell (2005), Retrieval of aerosol scattering and absorption properties from photopolarimetric observations over the ocean during the CLAMS experiment, *J. Atmos. Sci.*, **62**, 1093–1117.
- Chu, D. A., Y. J. Kaufman, C. Ichoku, L. A. Remer, D. Tanré, and B. N. Holben (2002), Validation of MODIS aerosol optical depth retrieval over land, *Geophys. Res. Lett.*, **29**(12), 8007, doi:10.1029/2001GL013205.
- Chylek, P., and J. Wong (1995), Effect of absorbing aerosols on global radiation budget, *Geophys. Res. Lett.*, **22**, 929–931.
- Coakley, J. A., Jr., and P. Chylek (1975), The two-stream approximation in radiative transfer: Including the angle of the incident radiation, *J. Atmos. Sci.*, **32**, 61–70.
- Deuzé, J. L., P. Goloub, M. Herman, A. Marchand, G. Perry, and D. Tanré (2000), Estimate of the aerosol properties over the ocean with POLDER, *J. Geophys. Res.*, **105**, 15,329–15,346.
- Deuzé, J. L., et al. (2001), Remote sensing of aerosols over land surfaces from POLDER-ADEOS-1 polarized measurements, *J. Geophys. Res.*, **106**, 4913–4926.
- Diner, D. J., et al. (1998), Multi-angle Imaging SpectroRadiometer (MISR) description and experiment overview, *IEEE Trans. Geosci. Rem. Sens.*, **36**(4), 1072–1087.
- Dubovik, O., and M. D. King (2000), A flexible inversion algorithm for retrieval of aerosol optical properties from sun and sky radiance measurements, *J. Geophys. Res.*, **105**, 20,673–20,696.
- Dubovik, O., B. N. Holben, Y. J. Kaufman, M. Yamasoe, A. Smirnov, D. Tanré, and I. Slutsker (1998), Single scattering albedo of smoke retrieved from the sky radiance and solar transmittance measured from ground, *J. Geophys. Res.*, **103**, 31,903–31,923.
- Dubovik, O., B. N. Holben, T. F. Eck, A. Smirnov, Y. J. Kaufman, M. D. King, D. Tanré, and I. Slutsker (2002a), Variability of absorption and optical properties of key aerosol types observed in worldwide locations, *J. Atmos. Sci.*, **59**, 590–608.
- Dubovik, O., B. N. Holben, T. Lapyonok, A. Sinyuk, M. I. Mishchenko, P. Yang, and I. Slutsker (2002b), Non-spherical aerosol retrieval method employing light scattering by spheroids, *Geophys. Res. Lett.*, **29**(10), 1415, doi:10.1029/2001GL014506.
- Eck, T. F., B. N. Holben, J. S. Reid, O. Dubovik, A. Smirnov, N. T. O'Neill, I. Slutsker, and S. Kinne (1999), Wavelength dependence of the optical depth of biomass burning, urban and desert dust aerosols, *J. Geophys. Res.*, **104**(D24), 31,333–31,350.
- Eck, T. F., B. N. Holben, O. Dubovik, A. Smirnov, I. Slutsker, J. M. Lobert, and V. Ramanathan (2001), Column-integrated aerosol optical properties over the Maldives during the northeast monsoon for 1998–2000, *J. Geophys. Res.*, **106**(D22), 28,555–28,566.
- Eck, T. F., et al. (2005), Columnar aerosol optical properties at AERONET sites in central eastern Asia and aerosol transport to the tropical mid-Pacific, *J. Geophys. Res.*, **110**, D06202, doi:10.1029/2004JD005274.
- Geogdzhayev, I. V., M. I. Mishchenko, W. B. Rossow, B. Cairns, and A. A. Lacis (2002), Global two-channel AVHRR retrievals of aerosol properties of the ocean for the period of NOAA-9 observations and preliminary retrievals using NOAA-7 and NOAA-11 data, *J. Atmos. Sci.*, **59**, 262–278.
- Ginoux, P., M. Chin, I. Tegen, J. Prospero, B. Holben, O. Dubovik, and S.-J. Lin (2001), Sources and distributions of dust aerosols simulated with the GOCART model, *J. Geophys. Res.*, **106**(D17), 20,225–20,273.
- Gordon, H. R., and M. Wang (1994), Retrieval of water-leaving radiance and aerosol optical thickness over the oceans with SeaWiFS: A preliminary algorithm, *Appl. Opt.*, **33**, 443–452.
- Hansen, J. E., and L. D. Travis (1974), Light scattering in planetary atmospheres, *Space Sci. Rev.*, **16**, 527–610.
- Hansen, J. E., M. Sato, and R. Ruedy (1997), Radiative forcing and climate response, *J. Geophys. Res.*, **102**(D6), 6831–6864.
- Hartley, W. S., and P. V. Hobbs (2001), An aerosol model and aerosol-induced changes in the clear-sky albedo off the east coast of the United States, *J. Geophys. Res.*, **106**(D9), 9733–9748.

- Haywood, J. M., S. R. Osborne, P. N. Francis, A. Keil, P. Formenti, M. O. Andreae, and P. H. Kaye (2003), The mean physical and optical properties of regional haze dominated by biomass burning aerosol measured from the C-130 aircraft during SAFARI 2000, *J. Geophys. Res.*, **108**(D13), 8473, doi:10.1029/2002JD002226.
- Herman, J. R., P. K. Bhartia, O. Torres, C. Hsu, C. Seflor, and E. Celarier (1997), Global distribution of UV-absorbing aerosols from Nimbus 7/TOMS data, *J. Geophys. Res.*, **102**(D14), 16,911–16,922.
- Higurashi, A., and T. Nakajima (1999), Development of a two channel aerosol retrieval algorithm on global scale using NOAA AVHRR, *J. Atmos. Sci.*, **56**, 924–941.
- Hobbs, P. V., J. S. Reid, R. A. Kotchenruther, R. J. Ferek, and R. Weiss (1997), Direct radiative forcing by smoke from biomass burning, *Science*, **272**, 1776–1778.
- Holben, B. N., et al. (1998), AERONET - A federated instrument network and data archive for aerosol characterization, *Rem. Sens. Environ.*, **66**, 1–16.
- Holben, B. N., et al. (2001), An emerging ground-based aerosol climatology: Aerosol optical depth from AERONET, *J. Geophys. Res.*, **106**(D11), 12,067–12,097.
- Holzer-Popp, T., M. Schroedter, and G. Gesell (2002), Retrieving aerosol optical depth and type in the boundary layer over land and ocean from simultaneous GOME spectrometer and ATSR-2 radiometer measurements, 1, Method description, *J. Geophys. Res.*, **107**(D21), 4578, doi:10.1029/2001JD002013.
- Husar, R. B., J. M. Prospero, and L. L. Stowe (1997), Characterization of tropospheric aerosols over the oceans with the NOAA advanced very high-resolution radiometer optical thickness operational product, *J. Geophys. Res.*, **102**(D14), 16,889–16,909.
- Ignatov, A., and L. Stowe (2000), Physical basis, premises, and self-consistency checks of aerosol retrievals from TRMM/VIRS, *J. Appl. Meteorol.*, **39**(12), 2259–2277.
- Ignatov, A., and L. Stowe (2002), Aerosol retrievals from individual AVHRR channels. Part I: Retrieval algorithm and transition from Dave to 6S radiative transfer model, *J. Atmos. Sci.*, **59**, 313–334.
- Intergovernmental Panel on Climate Change (IPCC) (2001), *Climate Change 2001: The Scientific Basis. Contribution of Working Group I to the Third Assessment Report of the Intergovernmental Panel on Climate Change*, edited by J. T. Houghton et al., 881 pp., Cambridge Univ. Press, New York.
- Junge, C. E. (1955), The size distribution and aging of natural aerosols as determined from electrical and optical measurements in the atmosphere, *J. Meteorol.*, **12**, 13–25.
- Kahn, R. A., B. J. Gaitley, J. V. Martonchik, D. J. Diner, K. A. Crean, and B. Holben (2005), Multiangle Imaging Spectroradiometer (MISR) global aerosol optical depth validation based on 2 years of coincident Aerosol Robotic Network (AERONET) observations, *J. Geophys. Res.*, **110**, D10S04, doi:10.1029/2004JD004706.
- Kalashnikova, O. V., and R. Kahn (2006), Ability of multiangle remote sensing observations to identify and distinguish mineral dust types: 2. Sensitivity over dark water, *J. Geophys. Res.*, **111**, D11207, doi:10.1029/2005JD006756.
- Kaufman, Y. J., D. Tanré, L. Remer, E. F. Vermote, A. Chu, and B. N. Holben (1997), Operational remote sensing of tropospheric aerosol over the land from EOS-MODIS, *J. Geophys. Res.*, **102**(D14), 17,051–17,068.
- Kaufman, Y. J., D. Tanré, O. Dubovik, A. Karnieli, and L. A. Remer (2001), Absorption of sunlight by dust as inferred from satellite and ground-based remote sensing, *Geophys. Res. Lett.*, **28**(8), 1479–1483.
- Kaufman, Y. J., I. Koren, L. A. Remer, D. Tanré, P. Ginoux, and S. Fan (2005), Dust transport and deposition observed from the Terra-Moderate Resolution Imaging Spectroradiometer (MODIS) spacecraft over the Atlantic Ocean, *J. Geophys. Res.*, **110**, D10S12, doi:10.1029/2003JD004436.
- Kiehl, J. T., and B. P. Briegleb (1993), The relative roles of sulfate aerosols and greenhouse gases in climate forcing, *Science*, **260**, 311–314.
- King, M. D., Y. J. Kaufman, D. Tanré, and T. Nakajima (1999), Remote sensing of tropospheric aerosols from space: Past, present and future, *Bull. Am. Meteorol. Soc.*, **80**(11), 2,229–2,259.
- Kirchstetter, T. W., T. Novakov, and P. V. Hobbs (2004), Evidence that the spectral dependence of light absorption by aerosols is affected by organic carbon, *J. Geophys. Res.*, **109**, D21208, doi:10.1029/2004JD004999.
- Knapp, K. R., T. H. Vonder Haar, and Y. J. Kaufman (2002), Aerosol optical depth retrieval from GOES-8: Uncertainty study and retrieval validation over South America, *J. Geophys. Res.*, **107**(D7), 4055, doi:10.1029/2001JD000505.
- Köepke, P., M. Hess, I. Schult, E. P. Shettle (1997), Global aerosol data set. MPI Meteorologie Hamburg Rep. 243, 44 pp.
- Léon, J.-F., D. Tanré, J. Pelon, Y. J. Kaufman, J. M. Haywood, and B. Chatenet (2003), Profiling of a Saharan dust outbreak based on a synergy between active and passive remote sensing, *J. Geophys. Res.*, **108**(D18), 8575, doi:10.1029/2002JD002774.
- Liu, H., and R. T. Pinker (2008), Radiative fluxes from satellites: Focus on aerosols, *J. Geophys. Res.*, doi:10.1029/2007JD008736, in press.
- Liu, H., R. T. Pinker, and B. N. Holben (2005), A global view of aerosols from merged transport models, satellite, and ground observations, *J. Geophys. Res.*, **110**, D10S15, doi:10.1029/2004JD004695.
- Lyapustin, A., D. L. Williams, B. Markham, J. Irons, B. Holben, and Y. Wang (2004), A method for unbiased high-resolution aerosol retrieval from Landsat, *J. Atmos. Sci.*, **61**(11), 1233–1244.
- Martonchik, J. V., D. J. Diner, R. Kahn, M. M. Verstraete, B. Pinty, H. R. Gordon, and T. P. Ackerman (1998), Techniques for the Retrieval of aerosol properties over land ocean using multiangle data, *IEEE Trans. Geosci. Remote Sens.*, **36**, 1212–1227.
- Martonchik, J. V., D. J. Diner, R. Kahn, B. Gaitley, and B. N. Holben (2004), Comparison of MISR and AERONET aerosol optical depths over desert sites, *Geophys. Res. Lett.*, **31**, L16102, doi:10.1029/2004GL019807.
- Mie, G. (1908), Contribution to the optical properties of turbid media, in particular of colloidal suspensions of metals, *Ann. Phys. (Leipzig)*, **25**, 377–452.
- Mishchenko, M. I., I. V. Geogdzhayev, B. Cairns, W. B. Rossow, and A. A. Lacis (1999), Aerosol retrievals over the ocean by use of channel 1 and 2 AVHRR data: Sensitivity analysis and preliminary results, *Appl. Opt.*, **38**(36), 7325–7341.
- Mishchenko, M. I., J. W. Hovenier, and L. D. Travis (2000), *Light Scattering by Nonspherical Particles: Theory, Measurements and Applications*, Acad. Press, San Diego, 690 pp.
- Nakajima, T. Y., T. Nakajima, M. Nakajima, H. Fukushima, M. Kuji, A. Uchiyama, and M. Kishino (1998), Optimization of the Advanced Earth Observing Satellite II global imager channels by use of radiative transfer calculations, *Appl. Opt.*, **37**, 3149–3163.
- Nakajima, T., A. Higurashi, K. Aoki, T. Endoh, H. Fukushima, M. Toratani, Y. Mitomi, B. G. Mitchell, and R. Frouin (1999), Early phase emphasis of OCTS radiance data for aerosol remote sensing, *IEEE Trans. Geosci. Remote Sens.*, **37**, 1575–1585.
- O'Neill, N. T., T. F. Eck, B. N. Holben, A. Smirnov, and O. Dubovik (2001), Bimodal size distribution influences on the variation of Angstrom derivatives in spectral and optical depth space, *J. Geophys. Res.*, **106**(D9), 9787–9806.
- Patterson, E. M., D. A. Gillette, and B. Stockton (1977), Complex index of refraction between 300 and 700 nm for Saharan aerosols, *J. Geophys. Res.*, **82**(21), 3153–3160.
- Penner, J. E., R. E. Dickinson, and C. A. O'Neill (1992), Effects of aerosol from biomass burning on the global radiation budget, *Science*, **256**, 1432–1434.
- Prospero, J. M., P. Ginoux, O. Torres, S. E. Nicholson, and T. E. Gill (2002), Environmental characterization of global sources of atmospheric soil dust identified with the Nimbus 7 Total Ozone Mapping Spectrometer (TOMS) absorbing aerosol product, *Rev. Geophys.*, **40**(1), 1002, doi:10.1029/2000RG000095.
- Ramon, D., and R. Santer (2001), Operational remote sensing of aerosols over land to account for directional effects, *Appl. Opt.*, **40**, 3060–3075.
- Reid, J. S., T. Eck, S. Christopher, O. Dubovik, R. Koppmann, D. Eleuterio, B. Holben, E. Reid, and J. Zhang (2005), A review of biomass burning emissions Part III: Intensive optical properties of biomass burning particles, *Atmos. Chem. Phys.*, **5**, 827–849, SRef-ID: 1680-7324/acp/2005-5-827.
- Remer, L. A., and Y. J. Kaufman (1998), Dynamic aerosol model: Urban/industrial aerosol, *J. Geophys. Res.*, **103**(D12), 13,859–13,871.
- Remer, L. A., et al. (2005), The MODIS aerosol algorithm, products and validation, *J. Atmos. Sci.*, **62**(4), 947–973.
- Ross, J. L., P. V. Hobbs, and B. Holben (1998), Radiative characteristics of regional hazes dominated by smoke from biomass burning in Brazil: Closure tests and direct radiative forcing, *J. Geophys. Res.*, **103**(D24), 31,925–31,941.
- Russell, P. B., J. M. Livingston, P. Hignett, S. Kinne, J. Wong, A. Chien, R. Bergstrom, P. Durkee, and P. V. Hobbs (1999), Aerosol-induced radiative flux changes off the United States Mid-Atlantic coast: Comparison of values calculated from sunphotometer and in situ data with those measured by airborne pyranometer, *J. Geophys. Res.*, **104**(D2), 2289–2307.
- Salomonson, V. V., W. L. Barnes, P. W. Maymon, H. E. Montgomery, and H. Ostrow (1989), MODIS: Advanced facility instrument for studies of the Earth as a system, *IEEE Trans. Geosci. Remote Sens.*, **27**, 145–153.
- Satheesh, S. K., and V. Ramanathan (2000), Large differences in tropical aerosol forcing at the top of the atmosphere and Earth's surface, *Nature*, **405**, 60–63.
- Satheesh, S. K., and J. Srinivasan (2005), A method to infer short wave absorption due to aerosols using satellite remote sensing, *Geophys. Res. Lett.*, **32**, L13814, doi:10.1029/2005GL023064.

- Schwartz, S. E. (1996), The Whitehouse effect-short-wave radiative forcing of climate by anthropogenic aerosols: An overview, *J. Aerosol Sci.*, **27**, 359–382.
- Shettle, E. P., and R. W. Fenn (1979), Models of aerosols of lower troposphere and the effect of humidity variations on their optical properties. AFCRL Tech. Rep. 79 0214, Air Force Cambridge Research Laboratory, Hanscom Air Force Base, MA, 100 pp.
- Sokolik, I. N., and O. B. Toon (1999), Incorporation of mineralogical composition into models of the radiative properties of mineral aerosol from UV to IR wavelengths, *J. Geophys. Res.*, **104**(D8), 9423–9444.
- Stowe, L. L., A. M. Ignatov, and R. R. Singh (1997), Development, validation and potential enhancement to the second generation operational aerosol product at the National Environmental Satellite, Data and Information Service of the National Oceanic and Atmospheric Administration, *J. Geophys. Res.*, **102**(D14), 16,923–16,934.
- Tanré, D., Y. J. Kaufman, M. Herman, and S. Mattoo (1997), Remote sensing of aerosol properties over oceans using the MODIS/EOS spectral radiances, *J. Geophys. Res.*, **102**(D14), 16,971–16,988.
- Torres, O., P. K. Bhartia, J. R. Herman, Z. Ahmad, and J. Gleason (1998), Derivation of aerosol properties from satellite measurements of backscattered ultraviolet radiation: Theoretical basis, *J. Geophys. Res.*, **103**(D14), 17,099–17,110.
- Torres, O., R. Decaie, P. Veefkind, and G. de Leeuw (2003), OMI aerosol retrieval algorithm, in *OMI Algorithms Theoretical Basis Document*, vol. 3, *Clouds, Aerosols and Surface UV Irradiance*, edited by P. Stammes, pp. 46–71, Neth. R. Meteorol. Inst., Utrecht.
- Torres, O., P. K. Bhartia, A. Sinyuk, E. J. Welton, and B. Holben (2005), Total Ozone Mapping Spectrometer measurements of aerosol absorption from space: Comparison to SAFARI 2000 ground-based observations, *J. Geophys. Res.*, **110**, D10S18, doi:10.1029/2004JD004611.
- Van de Hulst, H. C. (1957), *Light Scattering by Small Particles*, Wiley, pp. 414–418.
- Veefkind, J. P., G. de Leeuw, P. A. Durkee, P. B. Russell, P. V. Hobbs, and J. M. Livingston (1999), Aerosol optical depth retrieval using ASTR-2 and AFHRR data during TARFOX, *J. Geophys. Res.*, **104**, 2253–2260.
- Wang, J., S. A. Christopher, J. S. Reid, H. Maring, D. Savoie, B. N. Holben, J. M. Livingston, P. B. Russell, and S.-K. Yang (2003a), GOES 8 retrieval of dust aerosol optical thickness over the Atlantic Ocean during PRIDE, *J. Geophys. Res.*, **108**(D19), 8595, doi:10.1029/2002JD002494.
- Wang, J., S. A. Christopher, F. Brechtel, J. Kim, B. Schmid, J. Redemann, P. B. Russell, P. Quinn, and B. N. Holben (2003b), Geostationary satellite retrievals of aerosol optical thickness during ACE-Asia, *J. Geophys. Res.*, **108**(D23), 8657, doi:10.1029/2003JD003580.
- Whitby, K. T. (1978), The physical characteristics of sulphur aerosols, *Atmos. Environ.*, **12**, 135–159.
- Whitby, K. T., and B. K. Cantrell (1975), Atmospheric Aerosols - Characteristics and Measurement. ICESA Conference Proceedings, IEEE #75-CH 1004-1 ICESA, paper 29-1, 6 pp.
- Winker, D., J. Pelon, and M. P. McCormick (2002), The CALIPSO mission: Aerosol and cloud observations from space, in *21th International Lidar Radar Conference*, pp. 735–738, Int. Coord., Gr. on Laser Atmos. Stud., Québec, 8–10 July 2002.
- M. Chin and L. Remer, NASA Goddard Space Flight Center, Atmospheres Lab, Greenbelt, MD 20771, USA.
- B. Holben, NASA, Goddard Space Flight Center, Biospheric Sciences Branch, Greenbelt, MD 20771, USA.
- H. Liu and R. T. Pinker, Department of Atmospheric and Oceanic Science, University of Maryland, College Park, MD 20742, USA. (pinker@atmos.umd.edu)